



Title	Summary International Reports, September 1976, July 1977-June 1978
Citation	Memoirs of the Faculty of Engineering, Hokkaido University, 15(1), 101-133
Issue Date	1979-01
Doc URL	http://hdl.handle.net/2115/37965
Type	bulletin (other)
File Information	15(1)_101-134.pdf



[Instructions for use](#)

Fourth International Conference on
Port and Ocean Engineering under
Arctic Conditions September 26-30,
1977

Experimental Study one Ice Force on an Upright pile

Hiroshi SAEKI, Ken-ichiro HAMANAKA and Akira Ozaki
Department of Civil Engineering, Faculty of Engineering

Investigations were made on the ice force exerted on an isolated vertical pile. Three kinds of tests (test on the ice force with a newly developed test apparatus, field test on the ice force on an upright pile with a large diameter and tests on impulsive force) were carried out to obtain an experimental formula for the ice force on a pile.

Finally, authors proposed the experimental formula of ice force on a pile as follows

$$F = C \cdot \sqrt{W} \cdot h \cdot \sigma_c$$

F : ice force on a pile (kg), C : shape factor of pile which is 5.0 for a circular pile, 6.8 for a rectangular pile and 4.5 for a wedged pile with a wedge angle of 90° ($\text{cm}^{\frac{3}{2}}$), W : width of pile (cm), h : thickness of ice (cm), σ_c : uniaxial compressive strength (kg/cm^2)

International Symposium on Risk and
Reliability in Water Resources, Uni-
versity of Waterloo, Canada, June 26-
28, 1978

Incorporation of Forecasted Total Seasonal Runoff Volumes into Reservoir Management Strategies

Kiyoshi HOSHI

Research Associate, Dept. of Civil Engineering
Hokkaido University, Sapporo 060, Japan

Stephen J. BURGESS

Associate Professor, Dept. of Civil Engineering University
of Washington, Seattle, Washington 98195, U.S.A.

Forecasts of total snowmelt seasonal runoff volumes were used to determine operating rules for hypothetical reservoirs to determine the relative advantage of using forecasted flow over the unconditional flow state. Comparisons were made using chance constrained linear programming (CCLP) formulations for the operation of a single multiple purpose reservoir (flood mitigation, water supply, and hydropower generation) with and without snowmelt runoff forecasts. Two reservoir sizes, one approximately 20% and the other 100% of the mean annual flow of a river were examined. Flow

data from the Cedar River, Washington, were used to reflect runoff patterns typical of much of the Pacific Northwest region.

Conditional streamflow distributions for the months of March through August were developed for given total March-August runoff volume amounts. These conditional distributions were used to develop Linear Decision Rules (LDR's) for release from the reservoir. LDR's were also developed for the maximum ignorance state. Economic benefits were computed for maximum ignorance operating rules (Type A), Type A operating rules with conditional inflows (Type B), and LDR's and benefits based on the conditional flows (Type C). Generally, under Type C operation there was less uncertainty in the cumulative distributions of water supply and reservoir freeboard (surrogate for flood control) than when Type A operation was used. Explicit inclusion of the total seasonal runoff forecast into reservoir operation reduces physical operating uncertainty, as well as generates larger benefits than are determined by operating under circumstances of maximum ignorance, i. e., only unconditional streamflow distributions are available.

The Seventh International Symposium
on Transportation and Traffic Theory
August, 1977. Kyoto, JAPAN

A non-linear Traffic Model and Practical Capacity on Snowy and Icy Surfaces

Keiichi SATO* and Hideo IGARASHI**

A non-linear traffic model is studied in order to regress the experimental data collected on a rural two lane road in a summer and winter season. The major effort was given to establish the non-linear regression analysis to estimate the parameters of the non-linear expression for the traffic flow. The direct application of the non-linear regression analysis gave a considerably better level of the sum of the squared deviation than that obtained by the linear regression analysis. Some known traffic models are mathematically interrelated and derived from the general equation of the car following theory. The non-linear traffic flow model proposed in this paper, an Exponential non-linear model gave minimal deviations and the appropriate values of parameters.

The experimental data were analyzed by the Exponential non-linear model, and it was found that the practice capacity in winter is decreased by approximately 40% as compared with that in summer.

* Research Associate, Dept. of Civil Engineering

** Professor, Dr. Eng., Dept. of Civil Engineering

2nd International Symposium on Snow
Removal and Ice Control Research.
Hanover, New Hampshire May 14th-
May 19th 1978

A Study on the Resistance of Snowplowing and the Running Stability of Snow Removal Truck

Terutoshi KAKU

Current snowplowing of the road surface by a truck equipped with a snowplow in winter is being carried out at low speeds under 30 km/h. Recently, a demand for higher speed snowplowing has arisen in an attempt to cope with the increase in traffic. However only a few research papers on the resistance of snowplowing and running stability of snow removal truck are available. From the point of view described above, the present work deals with the resistance of snowplowing and the running stability of a snow removal truck at high speed. The resistance of snowplowing was obtained by the results from field experiments which were conducted by Hokkaido Development Bureau and the running stability of snow removal truck was derived by the calculation of the maximum speed of snow removal truck without any unstable motion on a tangent and curved road section.

Third International Symposium on the
Use of Computers for Environmental
Engineering Related to Building
10-12 May 1978, Banff, Canada

Some Aspects of the Effective and Natural Use of Solar Radiation in the Design of Houses

Kenzo SUZUKI and Noboru ARATANI
Department of Architecture, Faculty of Engineering

The purpose of this study is to demonstrate that there are large possibilities to reduce energy consumption in a living abode by the utilization of sufficient insulation and simple solar heating devices as well as by the use of mechanical solar heating systems.

One example of a solar house in Hokkaido is introduced. The house is highly insulated and has large windows facing south for the effective use of window solar heat gain. It also has a glazed roof which is used for heating air in the attic and for weather-proofing the solar water heater installed therein. Computer simulations show that the annual energy requirement in a solar house can be reduced by a factor of three, compared with a normal abode. Equations for predicting hourly solar radiation and the assessment of window sizes are included in the study.

Sheffield International Conference of
Solidification and Casting, July 18-21,
1977, Sheffield, England

The Effect of Fluid Flow on the Macrosegregation in Steel Ingots

Tadayoshi TAKAHASHI, Kiyoshi ICHIKAWA and Masayuki KUDOU

It is possible to understand quantitatively the macrosegregation in steel ingots if the flow velocity of bulk liquid during solidification can be obtained. It was found that the flow velocity of bulk liquid can be determined by applying Taylor's vortex flow to the solidification of carbon steel. As a result, the following relations are introduced,

$$Ke = 1 - (1 - k_0) S_h \quad \text{and} \quad U/V = 7500 S_h / (1 - S_h)$$

where Ke is the effective distribution coefficient defined as \overline{Cp}/C_{L_0} , \overline{Cp} is the average solute concentration of the dendrite and the interdendritic region, C_{L_0} is the solute concentration of bulk liquid, k_0 is the equilibrium distribution coefficient, S_h is the fraction of solid depending on the washing depth in the solid-liquid coexisting zone, U is the flow velocity of bulk liquid, and V is the solidification rate. The macrosegregation, *i.e.* Ke , is also theoretically explained on the basis of the mass transfer with turbulent mixing in the solid-liquid coexisting zone.

The International Corrosion Forum
Devoted Exclusively to the Protection
and Performance of Materials, March
6-10, 1978, Albert Thomas Convension
Center, Houston, Texas, U.S.A.

Corrosion Pretreatments for Copper-Zinc Alloys

G. W. POLING* and T. NOTOYA

Combinations of four different types of zinc-complexing agents with benzotriazole (BTA), an efficient complexant and corrosion inhibitor for copper, were tested as pre-treatment inhibitors for 70/30 and 60/40 brasses in aerated 3% NaCl solutions. Alkyl dithiocarbonates, of C₆ to C₈ chain length, proved superior to: 2,5-dimercapthotheadiazole (DMTDA); sodium diethyldithiocarbamate (DDC) and sodium diethyldithiophosphate (DEDTP), in combination with BTA under a variety of test conditions. Apart from acting as an acid inhibitor for 70/30 brass exposed to acidic NaCl solutions, the DMTDA was also an effective partner inhibitor for BTA. Combinations of the other two complexing agents (DDC and DEDTP) plus BTA actually accelerated the corrosion of 70/30

* University of British Columbia, Vancouver, B. C., Canada.

brass but provided good protection of 60/40 brass in the NaCl solutions. Scanning electron micrographs showing surface topographies of test specimens with and without these inhibitor pretreatments are presented. Galvanostatic polarization curves are shown to help evaluate the inhibiting action of each inhibitor combination.

Society of Automotive Engineers Technical Paper Series 780224 Presented at the Congress of SAE Cobo Hall, Detroit Feb. 27-March 3, 1978

Experimental Reduction of NO_x, Smoke, and BSFC in a Diesel Engine Using Uniquely Produced Water (0-80%) to Fuel Emulsion

Tadashi MURAYAMA, Minoru TSUKAHARA, Yasushi MORISHIMA
and Noboru MIYAMOTO

With the aid of a static mixer and nonionic emulsifying agent, a comparatively stable water-fuel emulsion was obtained. Engine performance in a 4 cycle direct injection engine using these fuels were studied.

A large reduction of NO_x concentration was obtained over a wide range of engine operation, in spite of the increased ignition lag and rapid combustion. Furthermore, economical improvements and reduction of exhaust smoke were obtained. The reduction of NO_x concentration, fuel consumption and smoke were even more remarkable when compared by operating the same engine with water fumigation.

International Symposium on Alcohol
Fuel Technology, November 21-23, 1977,
Wolfsburg, F. R. of Germany

Stratified Charge in a Single Chamber Engine Using Methanol

Ken-ichi ITO and Shuichi KAJITANI
Department of Mechanical Engineering, Hokkaido
University, Sapporo, Japan

Shoichi FUKAZAWA
Hokkaido Institute of Technology,
Sapporo, Japan

A stratified charge by means of direct auxiliary fuel injection was studied with a single chamber engine for the purpose of reduction of NO emissions without great sacrificing of fuel economy. The single cylinder S. I. engine was operated with a wide

open throttle at an engine speed of 1500 rpm, using a special shrouded spark plug as well as a conventional plug. Emissions and a number of engine performances were measured for various injection directions, overall equivalence ratios and injection rates, and for different values of injection ratio and injection timing. The results indicated that successful stratification was obtained with the auxiliary injection directly to the vicinity of the spark plug. Also the main fuel was carbureted. A reduction of over 50% NO emission was attained while maintaining the same thermal efficiency in comparison with non-stratified charge. This technique could not be applied to gasoline fuel because of spark plug fouling.

Proceedings of the XIth Conference
on "Dynamics of Machines", Prague,
Czechoslovakia, September 5-9, 1977

The Free Vibration of a Circular Plate Elastically Supported on Some Circular Arcs

T. IRIE and G. YAMADA

This paper presents a theoretical method to analyze the free vibration of a circular plate whose lateral deflection and rotation are elastically supported on some concentric circular arcs.

For this purpose, considering the reaction force and bending moment acting on the support as unknown harmonic force and moment, the stationary response of the plate to these loads is obtained. The unknown force and moment distributed along the support are expanded into Fourier sine series with unknown coefficients and the homogeneous linear equations concerning these coefficients are given in a matrix form by the use of restraint conditions on the supports. By obtaining the eigenvalues and eigenvectors of the matrix equation, the natural frequencies and the mode shapes of the plate are determined.

Applying the theory to a circular plate supported on two or four concentric circular arcs, the natural frequencies and the mode shapes are calculated numerically and presented in figures.

Sixth International Conference on Internal Friction and Ultrasonic Attenuation in Solids, Tokyo, July 4-7, 1977

Internal Friction in an Amorphous Ferromagnetic Alloy

Kōichi MUKASA and Masao MAEDA

Department of Electronics, Faculty of Engineering,
Hokkaido University

An amorphous $(\text{Co}_{88}\text{Fe}_{12})_{75}\text{Si}_{14}\text{B}_{10}$ ferromagnetic alloy was prepared by the roller quenching technique. Structural changes as a function of temperature were detected by DTA and X-ray diffraction. Precipitation of Co atoms in the amorphous phase occurs at 490°C and an amorphous phase begins to crystallize at 560°C.

The internal friction of the transverse vibration of a reed was measured on the specimen in amorphous state and the specimens annealed at 530°C and 700°C. It is possible to determine the thermal diffusivity from the location of the peak. A slight difference of the thermal diffusivity between the amorphous state and the crystalline state was observed, but the thermal diffusivity of the specimen annealed at 530°C was similar to that of the amorphous state. Young's modulus for the amorphous state is about 40% below the value for crystalline state.

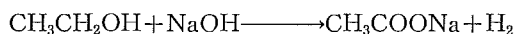
26th IUPAC Congress, 1977, 9 Tokyo,
Japan

Dissolution of Coal with the Treatment of Alcohol-NaOH

Koji OUCHI and Masataka MAKABE

The coal vitrits were reacted with 10 times of ethanol and NaOH. The products were extracted with pyridine and alcohol. The increase of NaOH amount increased the solubility. The yield of pyridine extract for younger coals is nearly 100% and it decreased in the higher rank of coal than 82% C. Ethanol extraction yield decreased from 70% of the younger coal to 10% of the oldest coal. The higher temperature than 260°C gave nearly 100% of solubility in pyridine for 1 hr reaction of Taiheiyo coal, but at 450°C it decreased slightly because of the polymerization reaction.

The reaction is mainly hydrolysis accompanying the hydrogenation with the hydrogen arising from the reaction as follows



The structural analysis of pyridine extract of Taiheiyo coal showed that its aromatic ring was benzene or naphthalene and $f_a = 0.7$.

International Conference on Heat
Measurement, 1977, 8 Kyoto, Japan

Application of High Pressure DTA Flow Method for Investigation of Fluidizing Reduction of Iron Ore

Sogo SAYAMA, Yoshinobu UEDA, Yasumori NISHIKAWA,
Shigeru UEDA, Shin-ichi YOKOYAMA
and Kazuo MAKINO

High pressure DTA equipment of gas flow type was used for the fluidizing reduction of iron ore. This DTA curve was measured with the conventional non isothermal method as well as with isothermal method. Mauntnewman hematite ore was used as a test sample.

The reduction became faster as the temperature rised. The effect of an increase of H₂ pressure on the reduction rate became negligibly small at a pressure higher than 15 kg/cm². The effect of H₂ pressure was relatively large at a lower temperature and a smaller gas flow rate. The rate of reduction generally increased with the increase of H₂ gas flow rate.

13th Biennial Conference on Carbon,
1977, 7 Los Angeles, U.S.A.

Carbonization of 3.5-dimethylphenol-formaldehyde Resin and its Chemical Structure at Mesophase Appearance

Yasumasa YAMASHITA and Koji OUCHI

3.5-dimethylphenol-formaldehyde resin (I) was carbonized and the evolved gases were analysed continuously. Dewater starts from 200°C attaining maxima at 300, 450 and 780°C. Demethanation starts from 250°C attaining maxima at 450 and 550°C. Carbon monoxide has a small maxima at 450, 600 and 780°C. Hydrogen evolves from about 400°C reaching its maximum at 700°C. From IR the first dewater reaction should be dewater from two OH groups or from OH and -CH₂-. The first demethanation may come from the evolution of methane from two neighbouring methyl groups and may form naphthene rings between the two benzene nuclei.

Most of the sample carbonized at 400°C could be dissolved in pyridine and its molecular weight was 1380. The structural analysis of this extract showed that its structure did not change so much from the original resin except the formation of few ether linkages and naphthene rings. The sample carbonized from 400°C to 430°C evolved only small amounts of gases and seemed to have nearly the same structure as that of 400°C, but this showed a mesophase. Therefore mesophase can appear from the large plane-like structure without a large aromatic condensed ring structure.

Gordon Research Conference, Fuel
Science, 1977, 7 Plymouth, U.S.A.

Mechanism of Hydrogenation of Coal Derived Asphaltene

Koji OUCHI

Asphaltene derived from Akabira coal was hydrogenated at 370°C or 400°C, with 22~23 MPa of working pressure, for 0~240 minutes, with red mud plus sulfur as the catalyst. The product was separated into unreacted asphaltene and oil. Structural analysis showed that the polymerization degree of unreacted asphaltene and oil increased with the conversion. The extrapolated value of oil is nearly the same as that of the starting asphaltene. Namely the splitting of the asphaltene molecules at the bridge parts linking the unit structures completely does not take place. The number of total, aromatic and naphthenic ring of unreacted asphaltene per unit structure showed nearly constant values whereas the number of total and aromatic ring per unit structure of oil decreased with conversion and that of naphthenic ring is constant. It is suggested from these facts that this reaction proceeded with the saturation of aromatic rings, opening of naphthenic or hetero rings and dehydroxylation.

International Conference on Heat
Measurement 1977, 8 Kyoto, Japan

Trial Manufacture of Flow Type High Pressure DTA Apparatus and its Application for Hydrogenolysis Reaction of coal

KAZUO MAKINO, Tomei TAKEGAWA and Koji OUCHI

High pressure flow type DTA apparatus was manufactured and its characteristics tested. This DTA uses a 1 cell detector, one thermocouple setting in the large heat capacity material and another in the sample. DTA is measured under a flow of gases, with the rising temperature or at a constant temperature.

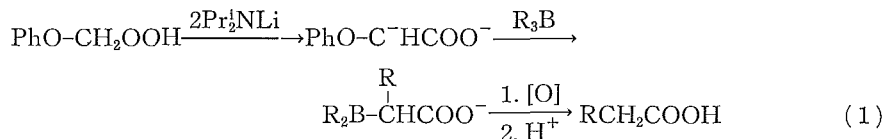
The characteristics of the apparatus were tested by supplying electric energy to a micro heater set in the sample.

One example of the application of this apparatus was the measurement of exothermic reaction of hydrogenolysis of coal at constant temperature. The exothermic reaction terminated in only 15 minutes and the area of this exothermic curve is proportional to the amount of water produced during this reaction. Namely the first reaction of hydrogenolysis of coal is a very rapid one and may be caused by the splitting of ether linkages.

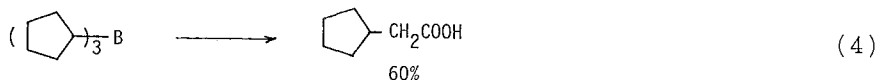
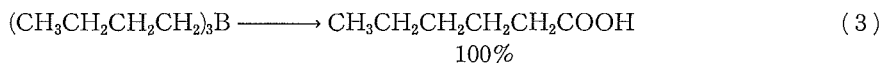
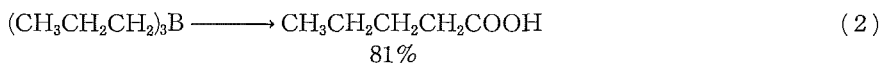
Direct Synthesis of Carboxylic Acids from Organoboranes

Shoji HARA, Kotaro KISHIMURA and Akira SUZUKI

In recent years, numerous reports have been published dealing with new syntheses of organic compounds from organoboranes. However, there are no reports on direct synthetic procedures for carboxylic acids, in spite of the fact that many efforts have been made to perform such syntheses. We wish to report here a convenient and direct synthesis of carboxylic acids by the reaction of organoboranes with the dianion of phenoxyacetic acid under mild conditions in relatively good yields (eq 1).



For example, a solution of tripropylborane in THF was added to a solution of the dianion formed from phenoxyacetic acid and lithium diisopropylamide in THF-ether. After refluxing the mixture for 2 hr, the intermediate thus obtained was oxidized with alkaline hydrogen peroxide, followed by acidification with hydrochloric acid. Glpc analysis revealed a 81% yield of pentanoic acid (eq 2). Some of the representative results obtained under such reaction conditions are shown in eqs 3 and 4.

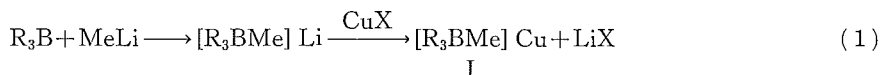


The 8th International Conference on
Organometallic Chemistry, Kyoto, Sep-
tember 12-16, 1977

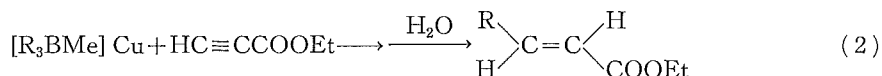
**The Reaction of Copper (I) Methyltrialkylborates with Ethyl
Propiolate and Ethyl β -Bromoacrylates. A Stereospecific
Synthesis of α,β -Unsaturated Carboxylic Acid
Esters from Organoboranes**

N. MIYAJURA, K. YAMADA, N. SASAKI,
M. ITOH and A. SUZUKI

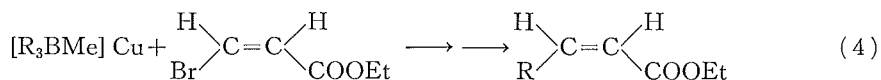
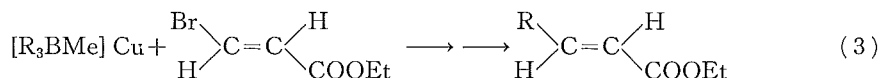
In the course of our studies on organic synthesis using copper (I) methyltrialkylborates (I) readily obtainable from lithium methyltrialkylborates and copper (I) halides (eq 1), we observed that these reagents react with ethyl propiolate, or β -bromoacrylates under mild conditions.



The reaction of ethyl propiolate with I gives corresponding addition products which are converted into α,β -unsaturated carboxylic esters in relatively good yields by hydrolysis. Such esters thus obtained are selectively trans-isomers (eq 2). Yields and purities of trans-isomers are markedly dependent upon the copper (I) halides and solvents employed. The reaction using copper (I) iodide as a halide and dimethoxyethane as a solvent gives the best results.



Such borate complexes (I) also react readily with β -bromoacrylates under the same reaction conditions to give corresponding unsaturated esters in good yields. When ethyl (E)- β -bromoacrylate is used, (E)- β -alkylacrylate is selectively obtained (eq 3). On the other hand, the (Z)- β -alkylacrylate is produced from the (Z)- β -bromoacrylate selectively (eq 4). This evidence seems to suggest that the reaction proceeds through the cis-addition and trans-elimination process.



26th International Congress of Pure
and Applied Chemistry, September
4-10, 1977 Tokyo, Japan

The Mechanism of the Transformation from Cellulose I to II

Jisuke HAYASHI, Takuji YAMADA and Mitsuo TAKAI

Mercerization is a typical transfer reaction from cellulose I to II in fibrous state. New crystal modifications, Na-cell VI, $1C_6H_{10}O_5 \cdot 1NaOH$ and Na-cell VII, $1C_6H_{10}O_5 \cdot 1NaOH \cdot H_2O$, were found in the course of the reaction, and the mechanism of the transformation was discussed.

Na-cell I from cell I or II was transformed to water-cell via Na-cell IV by washing with cold water and water-cell invariably gave cellulose II by drying. On the other hand, Na-cell I was transformed directly to cellulose I or II in a wet state, depending on its starting structure, via Na-cell VI. Boiling water removed first the water of crystallization from Na-cell I and changed it into Na-cell VI, and then removed NaOH to regenerate it into cellulose. In spite of the reaction in water, cellulose had no chance of hydration and was directly recrystallized. As the chain conformation of cellulose I or II type was not changed in this course, Na-cell I from cell I and II were regenerated into cell I and II respectively. Cold water readily removed NaOH from Na-cell I and formed a cellulose hydrate, water-cellulose. When the water was removed by drying, the chains are attracted by each other and should result in a twisted type conformation, cell II type.

It was concluded that the conformational change of the chain was due to hydration and dehydration which resulted in transformation from cell I to II.

2nd Joint Conference Chemical Institute of Canada, American Chemical Society, May 29-June 2, 1977 Montreal, CANADA

Mechanism of Transition Between Cellulose I and II

Mitsuo TAKAI and J. Ross COLVIN

Normally, the mercerization process with cellulose causes materials to swell but with the wet pellicle of bacterial cellulose, shrinkage occurs. Percentage shrinkages as high as 70% may be observed when the pellicle is allowed to mercerize freely at room temperature. The X-Ray diffraction pattern of the mercerized, washed, dried pellicle is essentially the same as that of Cellulose II. In contrast, high temperature mercerization ($\sim 100^\circ C$) results in shrinkages less than 10% and the diffraction pattern

remains the same as that of Cellulose I. With intermediate temperatures and pre-treatment of samples, the extent of shrinkage and conversion to Cellulose II show a hysteresis loop. No evidence was observed for "shishkebab" formation of lamellar Cellulose II in mercerization of bacterial cellulose microfibrils. It is suggested that the mechanism of mercerization of cellulose involves a progressive, relative shift of the sheets in the (200) plane of the crystallites of the microfibrils. This notion explains qualitatively all changes observed when Cellulose I transforms to Cellulose II. The shift need not and does not involve changes in the original polarity of the polyglucosan chains or solution of the cellulose. The mechanism may be applied equally well to those types of cellulose with anti-parallel structure as to those with parallel structure.

Cellulose, Paper and Textile Division
ACS Spring Meeting, May 17-19, 1978
at the Institute of Paper Chemistry
Appleton, Wisconsin, U. S. A.

Single Crystals of a Soluble Polyglucosan from *Acetobacter Xylinum*: Resemblance of Their Internal Structure to That of Cellulose Hydrate II

Mitsuo TAKAI and J. ROSS COLVIN

Hexahedral lamellar, single crystals are formed in water-methanol solutions at room temperature from an extracellular, water-soluble polyglucosan which is produced by *Acetobacter xylinum*, a cellulose-synthesizing bacterium. The crystals are very thin plates whose thickness is usually too small to estimate accurately by shadowing. Electron diffraction patterns of these plates show a typical, hexagonal symmetry. The observed reflections may be indexed on the basis of a hexagonal, two-dimensional unit cell with $a=b=5.18$ Å, $\gamma=120^\circ$. The third dimension of the unit cell can be obtained by 0-level Buerger precession X-ray photograph which shows $c=20.0$ Å, $\alpha=\beta=90^\circ$. Systematic absences of (0001) reflections were observed with $l=2n+1$. In general, X-ray diffraction patterns of the crystals are very similar to, if not identical with, the electron diffraction patterns. Both lead to the conclusion that the structure of the crystals is similar to that of Cellulose Hydrate II along the fiber axis. The chain axes lie parallel to the surface of the lamellar crystals and form sheets in the (0001) plane (i. e. the lamellar plane). From density data there appears to be 2.5 water molecules to every glucose residue and the water molecules lie in layers between the adjacent (0001) planes of the polyglucosan sheets.

Fifth International Conference on
Thermal Analysis, August 1-6, 1977,
Kyoto

**Thermoanalytical Study of the reactivity of Ferric Oxides
in the systems of α -Fe₂O₃-KClO₄ and α -Fe₂O₃-H₂**

Ryusaburo FURUICHI, Masahide SHIMOKAWABE and Tadao ISHII

Department of Applied Chemistry, Faculty of Engineering,
Hokkaido University, Sapporo, 060 Japan

DTA and TG experiments on the catalytic thermal decomposition of KClO₄ by α -Fe₂O₃ and the reduction of the oxide by H₂ were carried out to provide a clue to the change in reactivity of the oxide with the preparation history. α -Fe₂O₃ samples were prepared by the calcination of three iron salts at temperatures between 500°C and 1200°C in air. The initial decomposition temperature (T_{id}) of KClO₄ was 530°C, at which the fusion and the decomposition began simultaneously. The addition of α -Fe₂O₃ to KClO₄ (1:1 by wt.) resulted in a lowering of 30–110°C in T_{id} and a solid phase decomposition before the fusion of KClO₄. The values of T_{id} increased with an increase in the preparation temperature of α -Fe₂O₃. The initial reduction temperature (T_{ir}) of α -Fe₂O₃ changed from 260°C to 440°C with the increasing temperature of the preparation of α -Fe₂O₃. It was considered that the changes in reactivity of the oxide observed were due to the changes in degree of lattice order or defect with different preparation temperatures of α -Fe₂O₃.

Fifth International Conference on
Thermal Analysis, August 1-6, 1977,
Kyoto

**Thermoanalytical Study on the Solid-State Reactions
between Calcium Sulfate and Metal Oxides**

Tadao ISHII, Ryusaburo FURUICHI, Hiroaki MATSUSATO
and Takeshi OKUTANI

Department of Applied Chemistry, Faculty of Engineering,
Hokkaido University, Sapporo, 060 Japan

The thermal behaviour of CaSO₄ alone, CaSO₄-[oxide]_I, where [oxide]_I can be any one of MgO, CaO, ZnO, Co₃O₄, NiO or CuO and CaSO₄-[oxide]_{II} where [oxide]_{II} can be any one of Al₂O₃ (η , α), SiO₂ (amorphous, quartz), TiO₂ (anatase, rutile), Cr₂O₃, MnO₂ or α -Fe₂O₃, was studied in the temperature range 25–1400°C in a DTA apparatus in which the gas flows through the sample bed during the tests. In the CaSO₄-[oxide]_{II} systems, decomposition of CaSO₄ was promoted by the oxide presumably because of

the formation of binary metal oxides through some intermediate which is CaSO_4 incorporated with the oxide. On the other hand, in CaSO_4 -[oxide]_{II} systems the oxide had no effect on the decomposition of CaSO_4 . Isothermal kinetic experiments and scanning electron microscopy on the CaSO_4 -[oxide]_{II} systems showed that the CaSO_4 -[oxide]_{II} and CaCO_3 -[oxide]_{II} systems differ greatly in thermal behaviour and isothermal kinetics.

International Symposium Grain Dust
Explosions October 4-6, 1977 at Kansas
City, Missouri, U.S.A.

Evaluating Ignition Temperature, Minimum Explosive Limit and Flame Propagation Velocity

Tatsuo TANAKA ·
Dept. of Chem. Proc. Eng.

Experimental study of dust explosion has widely been carried out, but only a few theoretical studies have been available to date. The reason is that there are many independent factors influencing the explosion mechanism. The author has developed a model which enables one to evaluate theoretically the important items of dust explosion. As to the ignition point, the effect of the thermal radiation was taken into account: as a result, the different trend of the past experimental data on plastics and metals in terms of particle size was explained on a consistent basis.

Dynamic heat balance to the system, in which the particles are evenly distributed at the same distance apart, gave the minimum explosive limit concentration. From the distance between the two particles, one of which ignites and at the same instant the other is burnt out, the minimum explosive limit could be calculated. The theoretical evaluation is satisfactorily confirmed by experimental data.

Using the same arrangements of the particles in space the flame propagation velocity was computed for various dust concentrations and particle sizes. The calculated expansion rate of the gas evolved by the successive explosion showed that the flame propagation velocity was accelerated until a constant value is reached, the magnitude order of which was up to 50~60 m/s.

26th International Congress of Pure
and Applied Chemistry, Tokyo, 4-10
September 1977

X-ray Studies on the Structure of Polymers in Amorphous State

A. ODAJIMA, S. YAMANE and M. NUMAKAWA

Department of Applied Physics, Faculty of Engineering,
Hokkaido University

O. YODA and I. KURIYAMA

Takasaki Radiation Chemistry Research Establishment,
Japan Atomic Energy Research Institute, Takasaki

The radial distribution functions (RDF) of polyethylene (PE) amorphized by γ -ray irradiation, atactic polypropylene (a-PP) and ethylene-propylene random copolymers (EPRC) are obtained from the analyses of their observed X-ray intensity data in an attempt to examine the relationship between the molecular chain structure and the local ordering in the amorphous state. Decreasing the height of the first maximum by increasing the propylene fraction indicates less inter-chain ordering due to the substitution of the methyl group. However, the local ordering of EPRC at room temperature, is still higher than PE melts.

RDF curves of EPRC as well as amorphized PE exhibit broad maxima at ~ 5 Å, ~ 10 Å and ~ 15 Å as formed for polyethylene melt. On the other hand, a-PP exhibits quite different characteristics on the RDF, for instance, the 5 Å doubled maximum, which should be attributed to a more complicated intrachain structure than PE.

26th International Congress of Pure
and Applied Chemistry Tokyo, 4-10
September 1977

Fine Structure of Polyoxymethylene Crystals Formed in Radiation-Induced Solid State Polymerization

A. ODAJIMA, T. ISHIBASHI and H. NISHIJIMA

Department of Applied Physics, Faculty of Engineering,
Hokkaido University

Y. NAKASE and I. KURIYAMA

Takasaki Radiation Chemistry Research Establishment,
Japan Atomic Energy Research Institute, Takasaki

This paper describes the relationship between fine structures of polytrioxane (PTOX) and polytetraoxane (PTEOX) and their polymerization conditions, e. g., the polymeriza-

tion time, temperature and atmosphere.

The crystal size and lattice distortion in main- and sub-crystals in these crystals are determined. The extreme shrinkage of the longitudinal dimension in PTOX is attributed to internal strains in the extended-chain crystal, while the doubled peaks on the (001) profiles of PTEOX as-polymerized are indicative of the existence of two kind crystals with extended and lamellar morphologies.

The endothermic profile of them shows no evidence of the melting temperature difference between the main- and sub-crystals. PTOX with high polymer yield, however, indicates another endothermic peak at a higher temperature, which is attributed to superheating. The superheatability is reduced by γ -ray irradiation to less than 100 KR, which may be associated with only a limited amount of molecular scissions.

4th International Conference on Small-Angle Scattering of X-Rays and Neutrons, Gatlinburg, U.S.A., 3-7 October 1977

Determination of Void Structure of Polyoxymethylene Crystals Formed in Radiation-Induced Solid State Polymerization by Means of Small-Angle X-Ray Scattering

A. ODAJIMA, S. YAMANE, T. ISHIBASHI and E. WADA
Department of Applied Physics, Faculty of Engineering,
Hokkaido University

Small-Angle-X-Ray-Scatterings of polytrioxane and polytetraoxane, obtained by the γ -ray induced polymerizations in the solid state, indicate a sharp scattering extended along the equator, while no intense scattering in the meridian was seen except for polytetraoxane polymerized at more than 80°C. This finding is indicative of a strong alignment of needle-like voids lying inter fibres, especially in polytrioxane.

Absolute X-ray intensity measurements of polytrioxane perpendicular to its fibre axis suggest that micro-voids with 6% of a volume fraction are involved in it. The intensity data over a range of 2θ of $1'$ to 15° also allow us to calculate the radial size of voids, and give 200 Å on the average, while electron micrographs of polytrioxane exhibits closely packed long fibrils with a diameter of 200 to 1000 Å.

Futhermore, the radial size distribution function in a cylindrical system is derived in terms of the Mellin transformation method, and applied to the analysis of void scattering from polytrioxane.

International Symposium on Photo-
and Electro-Imaging, 26-30 September,
1977, Tokyo

Some Filtering Effects on the Reconstructed Image in Computed Tomography

Naoshi BABA and Kazumi MURATA

Department of Applied Physics, Faculty of Engineering,
Hokkaido University

It is beneficial to implement a filtering operation in the process of the image reconstruction from projection data. For the convolution algorithm in computed tomography, the filtering is readily done. Giving the suitable filter functions, it is possible to reconstruct, for example, contrast enhanced, noise or ringing suppressed, and edge sharpened images. By applying an apodization filter to the image reconstruction, side lobes of the point spread function can be reduced. We show that an apodization filter is also useful to suppress the halo-like radial noise structure which arises when the azimuthal sampling number of projections is insufficient. We also examine the performance of the filter for the contrast enhancement. The results are displayed by the flying spot scanner. Detailed discussions regarding these methods are presented.

79. Tagung der Deutschen Gesellschaft
für Angewandte Optik vom 16. bis 20.
Mai 1978, Berchtesgaden

Holographische Interferometrie mit 180°-Beobachtungsfeld und ihre Anwendung zur Rekonstruktion der Brechungsindex-Verteilung einer Luftströmung

Kazumi MURATA, Naoshi BABA und Kaoru KUNUGI

Department of Applied Physics, Faculty of Engineering,
Hokkaido University

Es wird ein neues holographisch-interferometrisches Verfahren vorgestellt, mit dem man das Interferenzmuster eines Phasenobjekts aus verschiedenen Richtungen beobachten kann. Weil jedes Interferenzmuster die in jeder Richtung integrierte Phase enthält, kann die dreidimensionale Verteilung des Brechungsindex im Objekt durch Computer numerisch rekonstruiert werden. Das Verfahren wird zur Messung der um einem Hitzdraht entstehenden Luftströmung angewandt.

ISP Commission I Symposium on Data
Acquisition and Improvement of Image
Quality and Image Geometry, 29-31
May, 1978, Tokyo

MTF Measurement of Photogrammetric Lenses

Kazumi MURATA*, Kazuo SAYANAGI** and Fumio KOGA***

Uses of MTF for photogrammetric lenses are discussed. A new instrument for measuring of MTF of lenses mounted in photogrammetric cameras is constructed. Several cameras on the market are tested and the results are evaluated in detail.

5th International Conference on Crystal Growth, Boston, Mass., U.S.A.,
July 17-22, 1977

The Formation Mechanisms of Concentric Dislocation Loops in Ice Single Crystals Grown from the Melt

Mitsugu OGURO

Physics Laboratory, Asahikawa College, Hokkaido University
of Education, Asahikawa 070, Japan

Akira HIGASHI

Department of Applied Physics, Faculty of Engineering
Hokkaido University, Sapporo 060, Japan

Concentric dislocation loops with [0001] Burgers vectors were found by X-ray diffraction topography both in pure and impurity-doped ice single crystals grown from the melt. Although the abundance of the loops in NH₃-doped ice led us to conclude that the generation of the loops was an impurity effect, the real formation mechanism has not been made clear yet because of the lack of information regarding the types of the dislocation loops.

Experiments were carried out for the determination of the types (signs) of dislocation loops in ice by Chikaw's method in X-ray diffraction topography. All the loops in both pure and doped ice crystals were the interstitial type, regardless of the growth direction or of the species of the dopant. This result coincides with a theoretical prediction proposed by Fletcher on an idea of the structural diffusion in the liquid side near the growth interface.

The problem of nucleation of such interstitial type multiple dislocation loops at

* Department of Applied Physics, Faculty of Engineering, Hokkaido University, Sapporo

** Optics Research Division, Canon Inc., Tokyo

*** Geographical Survey Institute, Tokyo

or near growth interface are discussed quantitatively with an idea of the shear dislocations caused by minute misfitting inclusions and thermal stress. These inclusions are generated when minute unfrozen solute droplets are entrained at the interface due to the local instability and freeze behind the interface in the case of doped melt. Similar interpretation could be made for the case of pure ice.

Symposium on Physics and Chemistry
of Ice 1977, Cambridge, England
Sept. 11-16, 1977

Structure and Behavior of Grain Boundaries in Polycrystalline Ice

Akira HIGASHI

Department of Applied Physics, Faculty of Engineering
Hokkaido University, Sapporo 060, Japan

Recent progresses on studies of the structure and behavior of grain boundaries in ice are reviewed. As a lattice geometrical model of the boundary, the coincidence site lattice (CSL) model was considered with ice crystals. Some evidences of the validity of this model were presented through observations of special shapes of natural snow, results of grain boundary energy measurements and direct microscopic observations of boundaries by X-ray diffraction topography. Although methods of the measurement of grain boundary energy have been developed recently, results are still not sufficient to be analysed from real energetic standpoints with certain models of atomic bondings. A modern method of observing grain boundaries in ice using X-ray diffraction topography is described. Observations of migrating boundaries revealed that faceting along most closely packed CSL points impede the migration of the CSL boundaries whilst increased numbers of steps among facets with boundaries of other kinds enhance it. The mobility of the fast moving boundary has been determined to be in the order of $10^{-10} \text{ cm}^3 \cdot \text{dyne}^{-1} \cdot \text{sec}^{-1}$ either in a case of which driving force is a capillary force due to the boundary or in a case it is a stored energy of dislocations.

Symposium on Physics and Chemistry
of Ice 1977, Cambridge, England
Sept. 11-16, 1977

A Deformation Mechanism Map of Ice

Hitoshi SHOJI and Akira HIGASHI

Department of Applied Physics, Faculty of Engineering
Hokkaido University Sapporo 060, Japan

A deformation mechanism map for pure polycrystalline ice of 2 mm grain diameter is constructed. New sub-fields in the hitherto described dislocation glide field are proposed; dislocation glide with crack formation (DGC) upon dislocation creep and fracture at high stress level above the order of 1 MPa. The boundary between the dislocation creep and DGC is determined as the criterion of onset of cleavage cracks due to piled-up dislocations near grain boundaries. The fracture field is set on a basis of experimental fact that fracture occurs readily when the ice is subjected to a rapid deformation of which rate exceeds 10^{-3} sec^{-1} . Results of various experimental data on the stress dependence of the compressive deformation rate of polycrystalline ice are compared with the map. Effect of the change of activation energy of creep rate near the melting point is discussed as well as with those of other factors.

Symposium on Physics and Chemistry
of Ice 1977, Cambridge, England
Sept. 11-16, 1977

X-Ray Diffraction Topographic Observations of the Large Angle Grain Boundary in Ice under Deformation

Takeo HONDOH and Akira HIGASHI

Department of Applied Physics, Faculty of Engineering
Hokkaido University, Sapporo 060, Japan

Large angle tilt grain boundaries in artificially grown ice bicrystals were observed by the method of X-ray diffraction topography. In bicrystals of which misorientation angles satisfy the condition of high density coincidence sites, there appear images of fine parallel line defects on the topograph taken right after a light deformation. Since these images disappear in a duration between several hours and a few days and reappear again at the same sites when the specimen was deformed successively, it is concluded that those line defects are not stable like the intrinsic grain-boundary dislocations but may be the steps generated on the boundary to compose it with facets which lie parallel to the high density planes of the CSL. X-ray topographic images of the boundary of which misorientation angle does not satisfy the condition of high density

coincidence sites are complex and difficult to interpret, although some of them indicate that there may be some different sorts of structures on such boundaries.

The Electrochemical Society, Symposia
Meeting, Seattle, Washington, May 21-
26, 1978

Mechanism of 'Pore-Filling' of the Porous Oxide Films on Aluminium

H. TAKAHASHI, M. KODA and M. NAGAYAMA
Analytical Chemistry Laboratory, Faculty of Engineering
Hokkaido University, Sapporo, 060 Japan

Aluminium specimens anodized in an oxalic acid solution to form porous oxide films were re-anodized at a constant current density in a neutral boric acid-borate solution (pH=7.4). The pore-filling phenomenon occurring during the re-anodization was followed by electron microscopy using an ultra-thin sectioning technique and by potential measurement combined with chemical analysis of the solution. It was expected that the re-anodizing current is carried by the movement of Al^{3+} and O^{2-} ions across the barrier oxide layer to form new oxide at the oxide/solution and oxide/metal interfaces. Thus, pores of the porous layer are gradually filled with oxide. The increase in the applied voltage during the re-anodization directly reflects the increase in the barrier layer thickness. For a constant c. d., the voltage-time curve is a straight line whose slope decreases after the pore-filling is completed.

Analysis of the experimental results showed that the transport numbers for Al^{3+} and O^{2-} are 0.40 and 0.60. These figures vary only slightly with the re-anodizing c. d. in the range 0.05–0.5 mA/cm² but change remarkably with the solution composition.

The significance of the measured transport numbers is discussed in detail by comparing with those estimated from the marker experiments.

Fourth International Symposium on
Passivity, Airlie, Virginia, Oct. 17–21,
1977

XPS Studies on Anodic Oxide Films Formed on Iron in a Boric Acid-Borate Solution

H. KONNO and M. NAGAYAMA
Analytical Chemistry Laboratory, Faculty of Engineering
Hokkaido University, Sapporo, 060 Japan

The surface composition of passive oxide films formed anodically on iron in a boric

acid-borate solution (pH=8.43) was examined by XPS (X-ray photoelectron spectroscopy). A photoelectric cross-section ratio, $\sigma(\text{Fe } 2\text{P}_{3/2})/\sigma(\text{O } 1\text{s})$, of 1.65 determined with standard oxide samples was applied to the analysis of the photoelectron spectra. It was found that the outer part of the film is essentially composed of $\text{Fe}_2\text{O}_3 + \text{FeOOH}$ ($\text{OH}/\text{Fe}=0.3-0.5$) and some of Fe ions have valencies higher than 3+. The average Fe ion charge, $n+$, was measured to be 3.2-3.7, the existence of Fe^{6+} ions being occasionally indicated in the spectra. In addition to the chemically bound water, there is some water adsorbed weakly onto the surface, its amount increases with decreasing anode potential for potentials below 0 V (vs. SCE). For thin films formed at lower potentials, there is an indication that Fe^{2+} ions may exist in the inner part of the film. During the cathodic reduction of the anodized specimen, $n+$ decreased gradually through 3 to 2.6 in the first wave of the cathodic reduction curve. The latter value is characteristic of Fe_3O_4 . Sputter-etching of the anodized specimen with an Ar ion beam causes a drastic change in the surface composition, namely Fe_2O_3 is converted to a lower oxide such as FeO in a short time probably due to preferential sputtering. This was also ascertained with standard oxide samples. For this reason, it seems that examination of the composition in depth profile by XPS combined with Ar ion sputtering will give distorted results.

26th International Congress of Pure
and Applied Chemistry, Tokyo, Japan,
4-10 September, 1977

Highly Sensitive Spectrophotometric Determination of Cu^{2+} and Cd^{2+} with Water Soluble Porphines

Takao YOTSUYANAGI*, Jun-ichi ITO**, Shukuro IGARASHI*
and Kazuo AOMURA*

The simpler porphines and their metal complexes have an intense, well-defined absorption band (Soret band) in the spectrum at 390-460 nm, which has unusually large molar absorptivity (ϵ) of 2.5×10^5 to 5×10^5 . However, the Soret band of these compounds has not previously been utilized in analytical methods for the determination of metals. The only exceptions are those for Cu^{2+} and Pb^{2+} with $\alpha, \beta, \gamma, \delta$ -tetraphenylporphine-trisulphonate (TPPS). Banks and Bisque have also proposed the colorimetric method for Zn^{2+} with tetraphenylporphine (TPP), however, they used the absorption band in visible region only (at 551 nm $\epsilon: 1.4 \times 10^4$). The present study is concerned with the formation of the Cu^{2+} - $\alpha, \beta, \gamma, \delta$ -tetrakis (4-N-methylpyridyl)-porphine (TMPyP) complex and the Cd^{2+} -TPPS complex in aqueous solution and the preliminary investigation of analytical application to determine trace amounts of Cd^{2+} and Cu^{2+} spectrophotometrically.

*) Laboratory of Analytical Chemistry, Faculty of Engineering, Hokkaido University

***) Department of Organic Synthesis, Faculty of Engineering, Kyushu University

26th International Congress of Pure
and Applied Chemistry, Tokyo, Japan,
September 4-10, 1977

The Role of Semiquinone Anion in the Photoreduction of p-Benzoquinone in Ethanol

Shoji NODA, Toshihiko MIZUTA and Hiroshi YOSHIDA

The photoreduction of p-benzoquinone into hydroquinone was studied in a dilute ethanol solution at room temperature, by means of the spectrophotometric method. By exciting the quinone at its $\pi^* \leftarrow n$ (435 nm) and $\pi^* \leftarrow \pi$ bands with monochromatized light, the quinone concentration decreases and the hydroquinone concentration increases linearly with the number of absorbed photons. The quantum efficiencies are 0.24 and 0.22 for the quinone decay and the hydroquinone formation, respectively, for the $\pi^* \leftarrow n$ excitation. They are 0.36 and 0.30 for the $\pi^* \leftarrow \pi$ excitation. Combined with the previous ESR studies on the behavior of semiquinone intermediates detected during the photolysis, the present results give firm evidence for the anionic mechanism in the photoreduction of the quinone into the hydroquinone: the semiquinone anion primarily formed by the one-electron transfer from solvent ethanol to the excited quinone is responsible for the formation of the final photoproduct hydroquinone.

The First Japan-USSR Corrosion Seminar,
5-11 December, 1977, Moscow,
USSR

Passivity Breakdown and Pitting

Norio SATO

Electrochemistry Laboratory, Faculty of Engineering,
Hokkaido University

This article deals with some of the key points of local passivity breakdown and pitting corrosion. Those anions which destroy the short range water structure have a tendency to produce passivity breakdown. It is likely that the passive film is dynamically breaking down and repairing irregardless of the environment. The micro-breakdown of passive film is a stochastic process and the breakdown size distribution and rate are controlled by both the film destroying anions and the breakdown toughness of the film. The pit generation is determined by both the micro-breakdown of the film with the breakdown size larger than a critical value and the mass transport at the breakdown site. The stability criterion for pitting dissolution is represented by a critical breakdown intensity, which is the product of pit dissolution current density and pit size.

The Fourth International Symposium
on Passivity, 17-21 October, 1977. The
Airlie House Conference Centre, War-
renton, Virginia, U.S.A.

An Ellipsometric Study of Passivation Films on Cobalt in Neutral Borate Solution

Kiyokatsu KUDO, Norio SATO and Toshiaki OHTSUKA
Electrochemistry Laboratory, Faculty of Engineering
Hokkaido University

Passive films on cobalt formed by potentiostatic oxidation in a borate buffer solution were studied by means of ellipsometry combined with a cathodic reduction technique. Cobalt showed primary and secondary passivity depending upon the oxidation potential. In the primary passivity region cobalt was covered with CoO film whose thickness was of the order of 2.3 nm. In the secondary passivity region the film developed into a bilayered structure: an inner CoO and an outer Co_3O_4 layer. The outer layer thickened up to 3.7 nm almost linearly with the potential while being accompanied by a transition from Co_3O_4 to Co_2O_3 , and retained this thickness in the potential region where the transpassive dissolution took place. The inner layer also thickened with the potential in the secondary passivity region, but had a maximum thickness of about 4 nm at a potential near that where the transition from Co_3O_4 to Co_2O_3 occurs.

The Fourth International Symposium
on Passivity, 17-21 October, 1977. The
Airlie House Conference Centre, War-
renton, Virginia, U.S.A.

Bipolar Fixed Charge-Induced Passivity

Masao SAKASHITA and Norio SATO
Electrochemistry Laboratory, Faculty of Engineering
Hokkaido University

The paper presents a passivation mechanism in which the fixed ionic charge in a hydrous oxide deposit on metals plays an important part in producing passivity. If a hydrous oxide film consists of an anion-selective layer on the metal side and a cation-selective layer on the solution side, there arises a rectification of ion movement retarding the ionic current in the anodic direction, which eventually results in dehydration of the deposit film producing anodic passivation. Experimental evidences are shown for the rectification of ionic current through bipolar membranes of hydrous nickel (II) oxide.

The Fourth International Symposium on Passivity, 17-21 October, 1977. The Airlie House Conference Centre, Warrenton, Virginia, U.S.A.

The Passivity of Metals and Passivating Films

Norio SATO

Electrochemistry Laboratory, Faculty of Engineering
Hokkaido University

This paper reviews the present state of understanding of metallic passivity in aqueous solutions. The anodic polarization curve characteristic for passivation differs in different metals and solutions. The passive film on metals is classified into five types; the adsorption film, the three-dimensional barrier film, the barrier film on a less protective layer, the barrier film covered with a hydrous deposit layer, and the barrier film covered with a porous layer. The general theory of passivity, which considers that passivity results from a change in the electrified interface layer structure between the metal and the solution, is discussed with three mechanistic theories predicting the possibility of electron-configuration-induced passivity, ionic space-charge-induced passivity, and bipolar fixed charge-induced passivity.

The First Japan-USSR Corrosion Seminar, 5-14 December, 1977, Moscow, USSR

The State of Understanding of Metallic Passivity

Norio SATO

Electrochemistry Laboratory, Faculty of Engineering
Hokkaido University

This review describes the present state of phenomenological and mechanistic understanding of the passivity of metals and alloys in the following five chapters; 1) Anodic polarization curves, 2) Passivation processes, 3) Passive films, 4) Dissolution of passive films, and 5) Theory of passivity. It is concluded that a general framework of the understanding of passivity and passivating films has been established, although many detailed problems remain to be studied.

The First Japan-USSR Corrosion Seminar, 5-14 December, 1977, Moscow, USSR

Ion-Selectivity of Precipitate Films Affecting Passivation and Corrosion of Metals; Bipolar Fixed Charge-Induced Passivity

Masao SAKASHITA and Norio SATO

Electrochemistry Laboratory, Faculty of Engineering
Hokkaido University

Hydrous iron (III) oxide membranes in neutral solutions are anion-selective but they turn to be cation-selective in the presence of adsorbed CrO_4^{2-} , MoO_4^{2-} and WO_4^{2-} ions. The membrane can therefore be bipolarized by adsorbing these anions onto one side of the membrane surfaces. Such a bipolar membrane exhibits a rectification of ion flow through the membrane. Experiments show that the anodic current flowing from an anion-selective surface to a cation-selective surface of the membrane is reduced by orders of magnitude in bipolar hydrated (III) and nickel (II) membranes as compared with the corresponding anodic current in the absence of bipolarity. Furthermore, increased anodic polarization of this bipolar membrane may result in the formation of dehydrated compact oxide layer.

The First Japan-USA Joint Symposium on Corrosion Problems in Light Water Reactors, 28 May-2 June, 1978, Fuji Institute of Educational and Training, Susono, Japan

Introductory Remark to High Temperature Water Corrosion of Iron Base Alloys

Norio SATO

Electrochemistry Laboratory, Faculty of Engineering
Hokkaido University

This article describes a few fundamental concepts which are of importance in understanding the high temperature water corrosion of iron-based alloys. Firstly, the thermodynamic stability of iron and other alloying metals is illustrated in the potential/pH diagram, which is the basic standpoint of corrosion investigation. Secondly, the two apparently different corrosion mechanisms that are expected to operate on the metal surface in high temperature water are described; namely the electrochemical corrosion and the chemical corrosion. The third concept is the localization of corrosion which usually results from either local acidification or basification of environmental solution

at particular places on the metal surface determined by thermal-hydraulic conditions, solid deposits, and non-homogeneous surface composition of alloys. Finally, the effects of the metallurgical condition on corrosion are briefly discussed.

The 26th International Congress of
Pure and Applied Chemistry, 4-10 Sep-
tember, 1977, Tokyo, Japan

Ion-Selectivity in Corrosion Product Membranes: Fixed Charge on Hydrated Iron (III) Oxide

Masao SAKASHITA and Norio SATO
Electrochemistry Laboratory, Faculty of Engineering
Hokkaido University

The fixed charge on metal oxide precipitate membranes depends on the charge distribution at the oxide/solution interface. The membrane potential arising across hydrated iron (III) oxide precipitate membranes was measured and the effects of pH on the ion-selectivity was discussed. The membranes were anion-selective in chloride solutions less basic than pH 10.3 and cation-selection in more basic chloride solutions. The specific pH at which the ion-selectivity is reversed and hence the fixed charge vanishes is named the point of iso-selectivity pH_{pis} . This pH was found inconsistent with the point of zero charge pH_{pzc} , suggesting that the fixed charges are somewhat different from the surface charge.

The 27th Meeting of International
Society of Electrochemistry, 6-11 Sep-
tember, 1976, Zürich, Switzerland

Stability of Anodic Oxide Films on Cobalt

Toshiaki OHTSUKA and Norio SATO
Electrochemistry Laboratory, Faculty of Engineering
Hokkaido University

The anodic oxidation and anodic oxide films of cobalt were studied in borate buffer solutions in the pH range from 7 to 11. The anodic polarization curve shows the active dissolution, primary passivity, secondary passivity, tertiary passivity, and transpassivation. It is also shown that the anodic oxide film is hydrated oxide of CoO in the primary passive region, bi-layered oxide $\text{CoO}/\text{Co}_3\text{O}_4$ in the secondary passive region, and bi-layered oxide of $\text{CoO}/\text{Co}_2\text{O}_3$ in the tertiary passive and transpassive regions. The dissolution current of the anodic oxide film in the secondary and tertiary passive regions is much smaller than that in the primary passive region. By cathodic reduc-

tion the outer CoO_3 layer is first converted to Co_3O_4 and then reduced further to hydrated Co^{2+} ions before the inner CoO layer is reduced to metallic cobalt.

6th International Conference on Internal Friction and Ultrasonic Attenuation in Solids, Tokyo, July 4-7, 1977

Elastic Surface Wave Attenuation by Surface Inhomogeneities

Tsuneyoshi NAKAYAMA, Masa-aki NARITA and Tetsuro SAKUMA

Real surfaces are not ideal and contain many defects, such as chemisorbed impurities or surface roughness. Elastic surface wave (ESW) suffers the unavoidable attenuation considerably from these inhomogeneities. We investigate here theoretically the ESW attenuation due to the localized fluctuations of the mass density and the Lamé coefficients near the crystal surface. When the wavelength λ of the ESW is longer compared with the correlation length l characterizing the surface inhomogeneities, all contribution to the attenuation rate are proportional to the fifth power of the frequency. When λ is comparable to or smaller than l , attenuation constant varies more slowly with frequency. Numerical results will be presented for the frequency and correlation length dependence of the attenuation rate.

6th International Conference on Internal Friction and Ultrasonic Attenuation in Solids, Tokyo, July 4-7, 1977

Amplification of Ultrasonic Surface Mode Waves in a Piezoelectric Semiconductor Film

Sin-ichiro TAMURA and Tetsuro SAKUMA

Amplification characteristics of surface mode elastic waves in a piezoelectric semiconductor film are investigated quantum theoretically in the microwave frequency region, i. e., 10 to 100 GHz. We assume that the medium is isotropic elastically and that the effective mass approximation and a quasi-free description of the conduction electrons are valid. The deformation potential coupling and the piezoelectric coupling are considered as the sources of the electron-phonon interaction. We employ the Green's function method in the Born approximation to obtain the amplification rate. Numerical examples are developed for an n-type GaAs epitaxial layer on a semi-insulating GaAs substrate at 77 K. Frequency dependences of acoustic gains will be compared with those of the bulk wave and the surface (Rayleigh) wave.

6th International Conference on Internal Friction and Ultrasonic Attenuation in Solids, Tokyo, July 4-7, 1977

New Mechanism for the Kapitza Resistance

Tsuneyoshi NAKAYAMA

The acoustic mismatch (AM) theory of Khalatinikov is normally applicable in the range below about 0.1 K if allowance is made for phonon attenuation in the solid due to surface roughness or surface defects. Concerning the origin of the anomalous Kapitza resistance above about 0.1 K, although many investigations have been reported so far, the underlying mechanisms are still an open question. In the present work the contribution of tunneling states of helium atoms to the Kapitza resistance is theoretically investigated. It is shown the heat transfer is appreciably enhanced by the tunneling of the helium atoms close to the boundary. The efficiency of the heat transfer is shown to become rather strong for a temperature range above about 0.1 K. This theory is applicable to the case of the heat transfer between a solid and solidified He and H₂.

1977 IEEE Ultrasonics Symposium
Phoenix, October 26-28, 1977

Amplification of GHz Surface-Mode Acoustic Waves in a Piezoelectric Semiconductor Film

Shin-ichiro TAMURA and Tetsuro SAKUMA

Amplification characteristics of surface-mode acoustic waves in a piezoelectric semiconductor layer are investigated quantum theoretically in the GHz frequency region. We assume that the medium is elastically isotropic and that a quasi-free description of the conduction electrons is valid. The piezoelectric coupling is considered as the source of the electron-phonon interaction. We employ the Green's function method to obtain the amplification coefficients. The effect of the finite relaxation time of the conduction electrons is taken into account in the range of frequencies satisfying $\omega\tau < 1$. Numerical examples are developed for an n-type GaAs epitaxial layer on a semi-insulating GaAs substrate at 77 K. Frequency and drift parameter (applied field) dependences of acoustic gains will be illustrated and compared with those of the bulk wave.

1978 IEEE-MTT-S International Microwave Symposium, Ottawa, Ontario, Canada, June 27-29, 1978

Scattering Characteristics of a Beam Mode in Dielectric-Slab Optical Waveguide

M. IMAI*, S. MIYANAGA** and T. ASAKURA**

The amount and directivity of scattering light in a dielectric-slab optical waveguide, produced in a propagating beam mode due to refractive-index inhomogeneities of the thin film and due to boundary irregularities of film-air and film-substrate interfaces are calculated by means of a perturbation method together with the use of a stationary phase method.

The result of computer calculations shows the radiation pattern of scattered light due to these imperfections largely depends on the correlation length and variance of the wall perturbation and the refractive index inhomogeneities and on thin film thickness of a slab waveguide. In particular, the effect of the fluctuations of the refractive index is superior to that of the waveguide wall distortions in the radiated power into the air and substrate regions when $t/\lambda \geq 10.0$, where t is the thickness of a core region and λ is the wavelength of light.

The 10-th Symposium on Mathematical Physics, N. Copernicus University, Toruń, Poland, December 2-5, 1977

Rheonomic Cartan Spaces

Michiaki KAWAGUCHI

A Cartan space having its origin in the paper "Les espace de métriques fondés sur la notion d'aire" was developed by numerous workers, especially, L. Berwald. In the present paper we attempt to build up the geometry in this space from a standpoint of the rheonomic invariant theory. In this space, the (n-1)-dimensional area is assumed to be given a priori, in such a way that it depends on a variation of time. The geometrical quantities of this space depend on 4 kinds of parameters, x^a , t , u_a , u_o . If the time-area is independent of u_o , then in every moment this space reduces to a Cartan space in an ordinary sense, i. e. this area is nothing but that of a Cartan space. Since u_o may be interpreted as a velocity of a small piece of hypersurface-element, we shall call u_o a velocity of the hypersurface-element. As u_o is not invariant under a rheono-

* Department of Engineering Science, Hokkaido University

** Research Institute of Applied Electricity, Hokkaido University

mic transformation, we introduce an invariant parameter v in place of u_0 . This parameter v plays an important role in our theory. The form of the fundamental function $L(x^a, t, u_a, u_0)$ is rewritten in $G(x^a, t, u_a, v)$ which is a homogenous function of degree one in u_a and we decide the base connection, the connection-parameters, the curvature tensors and identities of Bianchi in our space.

U.S.-Japan Joint Conference on Continuum-Mechanical and Statistical Approaches in the Mechanics of Granular Materials, Sendai, Japan, June 5-9, 1978

A Geometrical Foundation of the Analysis of Granular Behavior

Masaru SHIMBO

This paper presents a microstructural formulation of the problem of the plastic behavior of granular materials in terms of non-Riemannian differential geometry. It is for the most part limited to static geometric analysis under the assumption of a small strain. This formulation covers rotation fields independent of that originating from the distribution of displacement. It reveals that a certain distribution of asymmetric stress entails the gradient of volumetric strain, affording a possible analytical representation of dilatancy in soil mechanics.

The 153rd Electrochemical Society
Seattle Meeting in May 21-26, 1978

High-Temperature Oxidation of Co-Mn Binary Alloys

K. NISHIDA, T. NARITA and S. KARASAWA

The purpose of this paper is to observe the morphology of the scale on Co-Mn alloys and consider the mechanism of scale formation on their alloys.

The results obtained are as follows :

- 1) The alloy up to 3% Mn has no formation of other oxide besides (Co, Mn)O mono-oxide, but a 6% Mn alloy shows massive (Co, Mn)₃O₄ spinel oxides formed in the outer part of matrix oxide at 1100°C in 1 atm oxygen. But a 17% Mn alloy shows a plate-like spinel oxide immediately inside massive spinel oxides of the scale.
- 2) The 17% Mn alloy oxidized at 1200°C in 1 atm shows no such platelike spinel oxide and has the appearance of 6% Mn alloy oxidized at 1100°C.
- 3) The same alloy oxidized at 1100°C in 10^{-1} atm shows no plate-like spinel oxide, containing only massive spinel oxides. In 10^{-2} atm and less this, the alloys have no

spinel oxide.

- 4) The above result can be partly explained by use of a Co-Mn-O phase diagram.

Pro. Fifth Int. Conf. on High Voltage
Microscopy, Kyoto, 1977

Application of HVEM to Reactor Materials

T. TAKEYAMA, H. TAKAHASHI and S. OHNUKI
Metals Research Institute, Faculty of Engineering
Hokkaido University, Sapporo, 060 Japan

High Voltage Electron Microscope (HVEM) has become one of the most suitable facilities for studying the simulation of radiation damage encountered in a nuclear reactor.

In this paper, as described below, four cases with regard to simulation experiments of defect behavior and interaction between solute atoms and point defects produced during irradiation by electrons, ions and neutrons were selected to illustrate some of the more recent studies of applications of HVEM to reactor materials;

- 1) Void swelling in electron-irradiated Ni (Interaction of point defects with dislocation.)
- 2) Void swelling in an electron-irradiated Ni-Cu alloy (Interaction of point defects with substitutional solute atoms).
- 3) Void formation in Pure iron by ion-irradiation.
- 4) Behavior of point defects on Fe-Mn-C alloys in neutron and electron irradiations.